Numerical Study of a Long-Lived, Isolated Wake Vortex in Ground Effect

Fred H. Proctor*
NASA Langley Research Center, Hampton, Virginia, 23314

This paper examines a case observed during the 1990 Idaho Falls Test program, in which a wake vortex having an unusually long lifetime was observed while in ground effect. A numerical simulation is performed with a Large Eddy Simulation model to understand the response of the environment in affecting this event. In the simulation, it was found that one of the vortices decayed quickly, with the remaining vortex persisting beyond the time-bound of typical vortex lifetimes. This unusual behavior was found to be related to the first and second vertical derivatives of the ambient crosswind.

Nomenclature

b_o	=	initial vortex separation (= $\pi B/4$)
B	=	wingspan of generating aircraft
IGE	=	in ground effect ($z < B$)
OGE	=	out of ground effect (vortex is away from any influence of ground)
r_c	=	radius of peak tangential velocity for initial vortex
t	=	time coordinate
T^*	=	nondimensional time (= $t\ V_o\ /\ b_o$)
u_c	=	ambient crosswind
V_o	=	initial vortex pair descent velocity (= $\Gamma_0 / (2\ \pi\ b_o)$)
x	=	horizontal coordinate in direction of flight path
y	=	horizontal coordinate orthogonal to direction of flight path
z	=	altitude, vertical coordinate
z_i	=	altitude of flight path, same as initial height of wake vortex
Z_P	=	altitude of port vortex
Z_S	=	altitude of starboard vortex
Z^*	=	nondimensional height (= z/b_o)
$\partial u_c/\partial z$	=	vertical shear of the environmental crosswind
$\partial^2 u_c/\partial z^2$	=	gradient of the crosswind shear
Γ	=	vortex circulation
Γ_0	=	initial vortex circulation
Γ^*	=	nondimensional vortex circulation (= $\Gamma\ /\ \Gamma_0$)
ζ_c	=	vorticity of crosswind (= $-\ \partial u_c/\partial z$)

I. Introduction

AIRCRAFT wake vortices can be a threat to trailing aircraft during all phases of flight (e.g., approach, departure, cruise, etc.). However, current standards and guidelines ensure sufficient separation between aircraft pairs to minimize this risk. Current research has focused on changing separation standards to allow greater capacity gains in the National Airspace System, while maintaining the current levels of safety and comfort. Reported incidences of wake encounters indicate that they occur during all phases of flight, but the majority of reports are associated with approach operations within the terminal airspace.[1] In this phase of flight it is particularly important to avoid encounters with wake turbulence, since aircraft are close to stall speed and have little time and airspace to recover from roll excursions or other unexpected accelerations. Wake encounters may be reported more frequently during

* Wake Vortex Tech Lead/POC, CSAOB, Mail Stop 152, AIAA Senior Member.

the final approach phase of flight because aircraft are operating along the same trajectory and wake vortices can rebound back into the flight corridor.

Decay rates of wake vortices are strongly enhanced following their maximum descent into ground effect.[2] This occurs because frictional drag, acting within the vortex-induced boundary layer, generates enhanced levels of turbulence. The flux of drag-induced turbulence then overwhelms the magnitudes of turbulence normally found in the environment. Therefore, not surprisingly, vortex decay while in ground effect (IGE) seems less sensitive to the intensity of environmental turbulence and stratification.[3] In the absence of environmental crosswind, Proctor et. al[2] has found that the conventional wake-vortex scaling rules seems to apply, and that normalized decay rates were insensitive to initial values of circulation, height, and vortex separation. Linear models of circulation decay based on ensembles of measured data do show a steeper rate of decay for IGE than for out of ground effect (OGE). As shown in Fig. 1, IGE wake decay rates, based on an exponential fit from Large Eddy Simulations (LES),[2] are in line with measurement-driven linear models of FAA-Eurocontrol data[4]. Concerns arise though, how vertical shear of the crosswind may affect the robustness of these models.

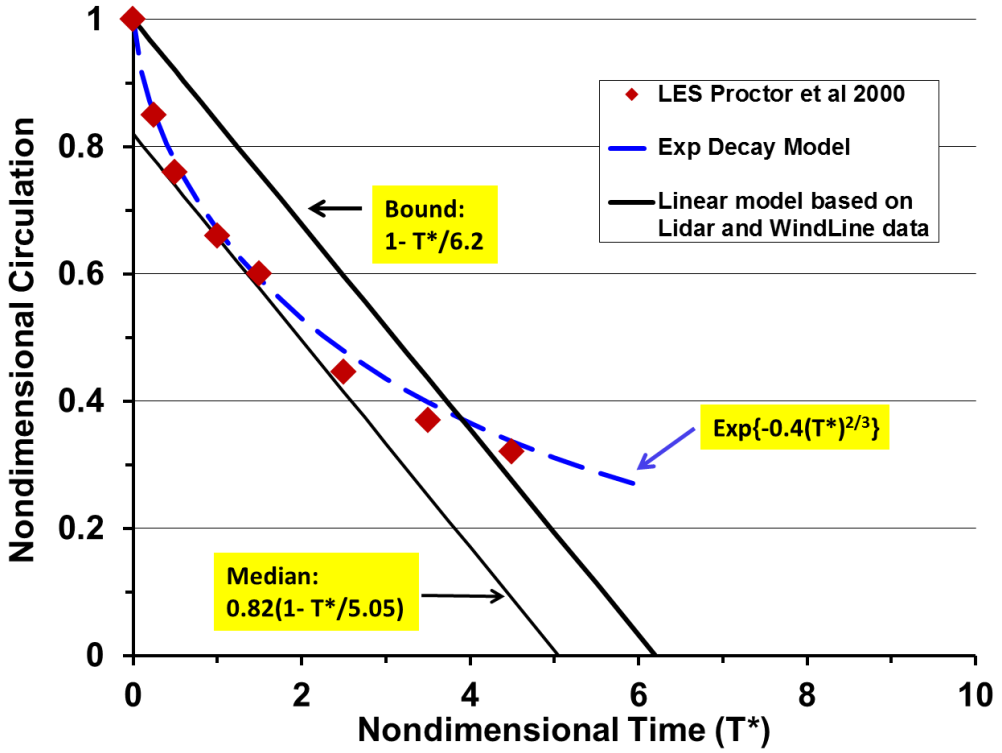

Figure 1. Circulation decay for a wake vortex in ground effect. Curve for exponential decay based on parametric numerical simulations with LES under conditions of calm mean winds.[2] Linear fits based on FAA-EuroControl Lidar and Windline measurments.[4]

Effects from crosswind shear may occur in IGE as well as OGE, and add complexity to predicting wake vortices. It has been shown that wake-vortex transport and decay are affected by the 1st and 2nd vertical derivatives of the environmental crosswind.[5] Complex and nonlinear gradients of windshear are common within the lowest elevations of the atmospheric boundary layer, owing to effects from surface drag and turbulence, as well as effects from surface heating and cooling.

The schematic in Fig. 2 illustrates how the tilt of a vortex pair is affected by the sign of the second derivative of the ambient crosswind (i.e., the vertical gradient of the crosswind shear). When the second derivative of the crosswind shear is negative, the clockwise-rotating port vortex (depicted by a plus sign) rises relative to the position of the counter-clockwise rotating starboard vortex (depicted by minus sign). If both the crosswind and crosswind shear are decreasing with height, the vortex pair will decrease in lateral separation (Fig. 2A) since the tilt exposes the higher downstream vortex to weaker crosswind. If the crosswind is decreasing with height and the crosswind shear is increasing with height, as in Fig. 2D, the vortex pair will increase in lateral separation since the tilt exposes the higher upstream vortex to weaker crossflow. For typical boundary layer wind profiles, Fig. 2B is the more

common profile, and we expect the downstream vortex to remain elevated and drift with increasing separation from the upstream vortex, as has been commonly observed.[6]

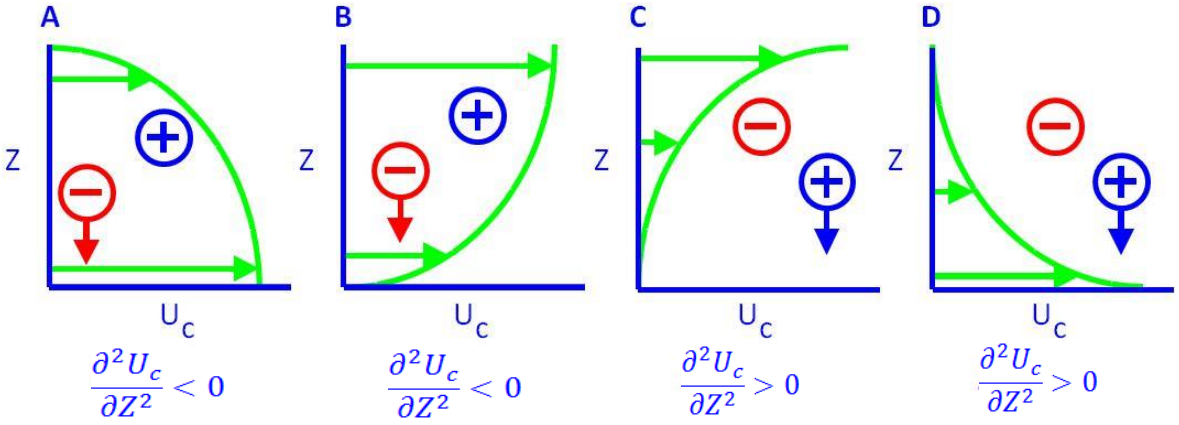

Figure 2. Schematic of crosswind shear effect on tilt of a wake vortex pair. Green curve represents vertical profile of crosswind (U_c). Wind distributions with a negative gradient of crosswind shear are shown in A) and B), while positive values are represented in C) and D). Wind distributions with negative values of wind shear ($\partial U_c/\partial z$) are represented in A) and C) while positive values in B) and D). Assuming a right-handed coordinate system directed along the aircraft path, the port vortex is represented by the red circle, and the starboard by the blue circle.

In addition to effects from the gradient of crosswind shear on vortex tilt, parametric studies assuming OGE conditions have shown that the shear of the crosswind determines whether the port or starboard vortex decays at a faster rate.[5] Results from this study are summarized in Table 1, with Z_s and Z_p representing the altitudes of the starboard and port vortex, respectively.

Table 1. Effect of crosswind shear on vortex pair.[5]

Depiction in Figure 2	$\partial^2 u_c/\partial z^2$	$\partial u_c/\partial z$	Tilt	Change in Lateral Separation (OGE)	Longest Lived Vortex
A	< 0	< 0	$Z_s > Z_p$	decreasing	starboard
B	< 0	> 0	$Z_s > Z_p$	increasing	port
C	> 0	> 0	$Z_s < Z_p$	decreasing	port
D	> 0	< 0	$Z_s < Z_p$	increasing	starboard
not shown	$= 0$	$\neq 0$	$Z_s = Z_p$	constant	same

Since the vorticity of the crosswind is simply, $\zeta_c = -\partial u_c/\partial z$, it is obvious from Table 1 that the longest lived vortices have the same sign of vorticity as that of the crosswind shear. For example in the scenario depicted in Fig. 2B, the port vortex tilts closest to the ground but the starboard vortex decays faster due to being immersed in vorticity that is countersign to its rotation. If the behavior depicted in Table 1 for OGE vortices holds during IGE, the scenario in Fig. 2B would result in the port (upstream) vortex descending deeper into ground effect, yet surviving longer than the starboard vortex. If the sign of the crosswinds were reversed ($u_c < 0$) without change in magnitude, then $\partial u_c/\partial z < 0$, and $\partial^2 u_c/\partial z^2 > 0$, and we would see the starboard (upstream) vortex descending deeper into ground effect and lasting the longest. The often used benchmark case, Idaho Falls B-757 Run 9, is a good example of this scenario, where the upstream vortex penetrated deepest into ground effect, yet lasted an unusually long time.[7,8,9,10]

Two examples of unusually long-lasting wakes from the 2012 FAA measurement campaign at JFK airport are shown in Figs. 3 and 4. Since the wake vortices from both the B-757 and the A-320 have nondimensional time units of ~20s, their wakes lasting longer that two minutes (i.e., $T^* > 6$) are unusual for IGE lifetimes (cf. Fig. 1). The environmental crosswind profiles for each of these cases is similar to that depicted in Fig. 2b, with both having

$\partial u_c/\partial z > 0$, and $\partial^2 u_c/\partial z^2 > 0$. From Table 1 we would expect the port vortex to last longer and to descend to a lower altitude, as is confirmed from the measurements depicted in Figs. 3 and 4.

The observation of unequal vortex decay rates is not unusual during field measurement campaigns; and in some instances, the differential decay has led to the occurrence of solitary vortices that have prolonged lifetimes (e.g., Idaho Falls flight test[7,8]). A solitary vortex would occur if one of the members of a vortex pair were to decay at a faster rate, leaving the remaining vortex as the sole survivor. The previously mentioned B-757 Run-9 case from the 1990 FAA-sponsored Idaho Falls tests is one example of this behavior, but other long-lived vortices have been observed as well.

In the Idaho Falls tests, B-727, B-757, and B-767 aircraft were flown at level flight upwind of a 200*ft* instrumented tower. Wake vortices were generated at ~70*m* altitude and quickly descended into ground effect while drifting through the tower. Each pass with each aircraft was given a run number, with the flights conducted for different aircraft configurations and for changing weather environments. Sensors for measuring wakes included anemometers mounted at 5*ft* increment on the 200*ft* tower, a Laser Doppler Velocimeter (LDV) Lidar, and a Monostatic Acoustic Vortex Sensing System.[7] Soundings for environmental temperature and wind were obtained from the instrumented tower and a tethered balloon. The long-lived vortices in some of the runs have been attributed to the unusual environment of Idaho Falls. One particular long-lived case can be identified as B-767, Run 23. In this run, the upstream vortex was observed to last over 2 *min* and 40*s*, while the downstream vortex was not detected after 60*s*. Thus the upstream vortex appeared to outlast than the downstream vortex by almost a factor of three. Two-dimensional simulations with the Terminal Areas Simulation System (TASS) have predicted a similar behavior for this event, including the early demise of the downstream vortex, but the reasons for the long-lived isolated vortex have yet to be identified.[8] In the remainder of this paper we will address a three-dimensional numerical simulation using the Idaho Falls B-767, Run 23 environment, observed at 0833 MDT on 30 September 1990. We have chosen to initialize our study with parameters representative of a B-747 rather than a B-767, due to the availability of an initial turbulence field for this case. Although the B-747 has a larger wingspan and stronger initial circulation than the B-767, both are heavies and should react similarly to the Idaho Falls environment of Run 23.

II. TASS Model

This study uses the Terminal Area Simulation System (TASS) which is a time-dependent LES model for simulating wake vortex and other aviation weather hazard phenomena.[8,11,12,13,14] The model has an initialization package that allows for the simulation of atmospheric wake vortices in the far-field, where environmental and ground surface interactions have important influences. The numerical model has: 1) a meteorological framework, 2) a realistic surface-stress formulation, 3) a subgrid turbulence-closure formulation with rotational damping of turbulence, and 4) a successful history in application to wake vortices.

Periodic boundary conditions are assumed for lateral boundaries, and the top boundary is selected to be impermeable and free slip. The bottom boundary is selected to represent a flat ground surface, with an impermeable nonslip velocity condition. Surface stress is modeled using Monin-Obukhov similarity theory, with ground stresses determined locally from the wind speed and thermal stratification. Details of the surface formulation are in Proctor and Han.[15]

The TASS model equations are discretized using quadratic-conservative fourth-order finite-differences in space for the calculation of momentum and pressure fields.[8] A third-order upstream-biased Leonard scheme[16] is used to calculate the transport of potential temperature and water vapor. A Monotone Upstream-centered Scheme for Conservation Laws (MUSCL)-type scheme after van Leer[17,18] is used for the transport of water substance. The TASS computational mesh uses the Arakawa C-grid staggering[19] for specifying velocities and thermodynamic quantities. The Klemp-Wilhelmson time-splitting scheme[20] is used for computational efficiency in which the higher-frequency terms are integrated by enforcing the CFL criteria to take into account sound wave propagation due to compressibility effects. The remaining terms are integrated using a larger time step that is appropriate for anelastic and incompressible flows. An Adams-Bashforth scheme is assumed for time differencing of momentum and pressure. Time steps are internally set and adjusted to meet numerical stability criteria. A sixth-order spatial filter is used to damp-out spurious oscillations in the velocity field that may arise due to the use of centered-differencing of momentum and pressure terms. Numerical tests have shown that the numerical formulation for the momentum and pressure equations in TASS is mass conservative and essentially free of numerical diffusion.[21]

Model domain parameters are listed in Table 2, and are chosen to give adequate resolution while maintaining a sufficiently large domain to minimize boundary influences.

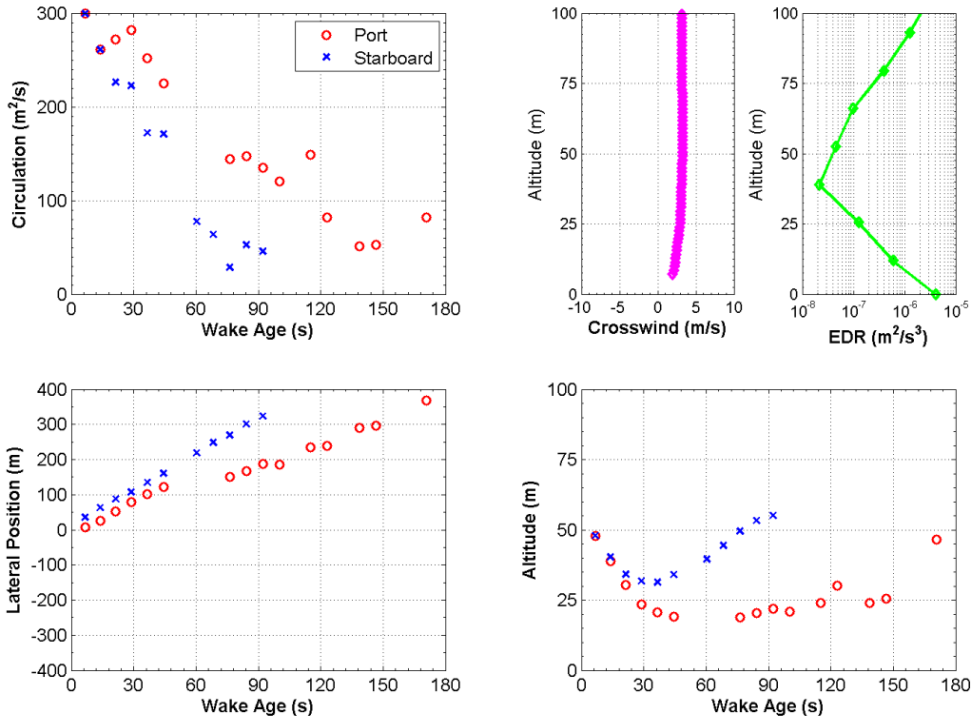

Figure 3. Measurements with pulsed Lidar for a B-757-200 at JFK airport (08/24/2012, 4:20 UTC). Wake positions and circulation are derived from Lidar measurements. Lidar sensed ambient profiles of crosswind and eddy dissipation rate (EDR) also shown at the top right. Data from FAA Wake Turbulence Program.

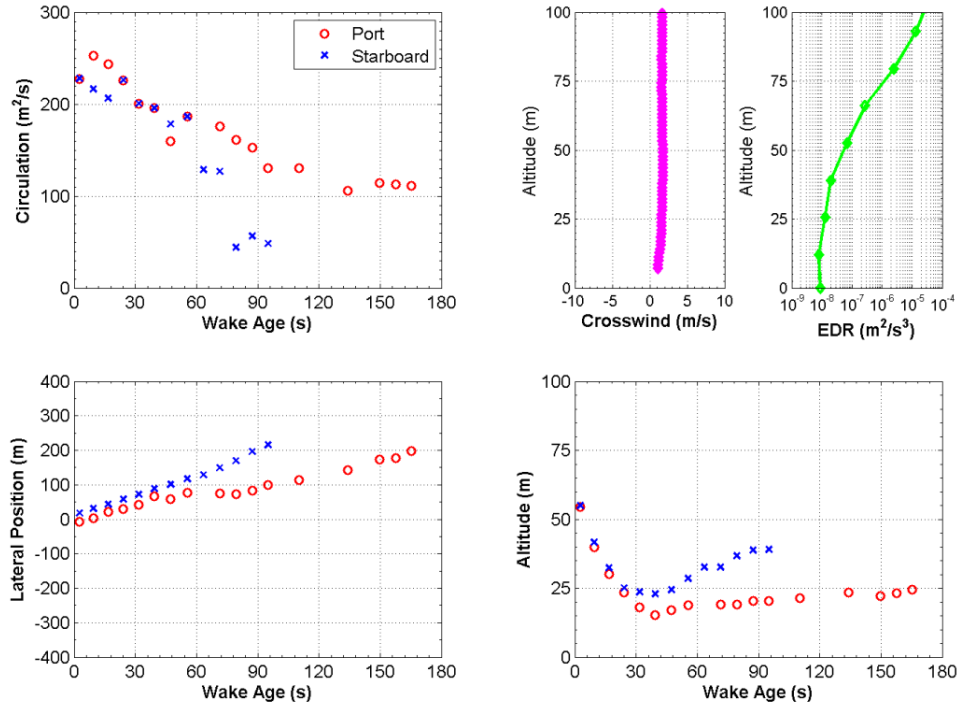

Figure 4. Measurements with pulsed Lidar for an A-320 at JFK airport (08/23/2012, 5:03 UTC). Wake positions and circulation are derived from Lidar measurements. Lidar sensed ambient profiles of crosswind and eddy dissipation rate (EDR) also shown at the top right. Data from FAA Wake Turbulence Program.

III. Initial Conditions

The initial vortex system is representative of a post roll-up, wake-vortex velocity field and consists of a pair of counter-rotating vortices that have no initial variation in the axial direction. Solutions for image vortices positioned outside of the domain are applied to guarantee consistency with boundary conditions. Parameters for the wake vortex initiation are listed in Table 3.

Table 2. Model domain parameters

Domain Size and Resolution	
Domain parameter	Physical dimension
Vertical dimension	450 *m*
Lateral dimension	800 *m*
Longitudinal dimension	400 *m*
Constant grid spacing	1.25 *m*

Table 3. Initial model parameters

Initial Vortex Parameters for TASS Simulations	
Aircraft class	Heavy (B-747)
Circulation (Γ_o)	565 $m^2 s^{-1}$
Vortex lateral separation (b_o)	50 *m*
Core radius (r_c)	3.75 *m* (= 3 grid points)
Height (z_i)	70 *m*
Vortex descent speed (V_o)	1.8 $m\ s^{-1}$

Resolved scale turbulence with an intensity of $10^{-5}\ m^2 s^{-3}$ is generated prior to the injection of wake vortices. This intensity of turbulence is weak, but appropriate for the stable environment. The initial crosswinds and potential temperature profile were obtained from measurement near the time of Idaho Falls, Run 23, and represent the environment for this event (Fig. 5). Note that the magnitude of crosswind below the flight path ($z_i = 70m$) is less than 2 *m/s* (Fig. 5A), and that the crosswind shear ($\partial u_c/\partial z$) and gradient of crosswind shear ($\partial^2 u_c/\partial z^2$) are both positive near the height of the flight path (Fig. 5B). From Table 1, we would expect the wake vortex pair to tilt upward toward the (upstream) port vortex, and that the port vortex should outlast the starboard vortex. The potential temperature profile in Fig. 5A shows the environment to be moderately stratified. An additional numerical simulation, described later, is initialized with a neutral lapse rate for temperature to determine what contribution the stable environment may have to the unusual behavior of the Idaho Falls Run 23 event.

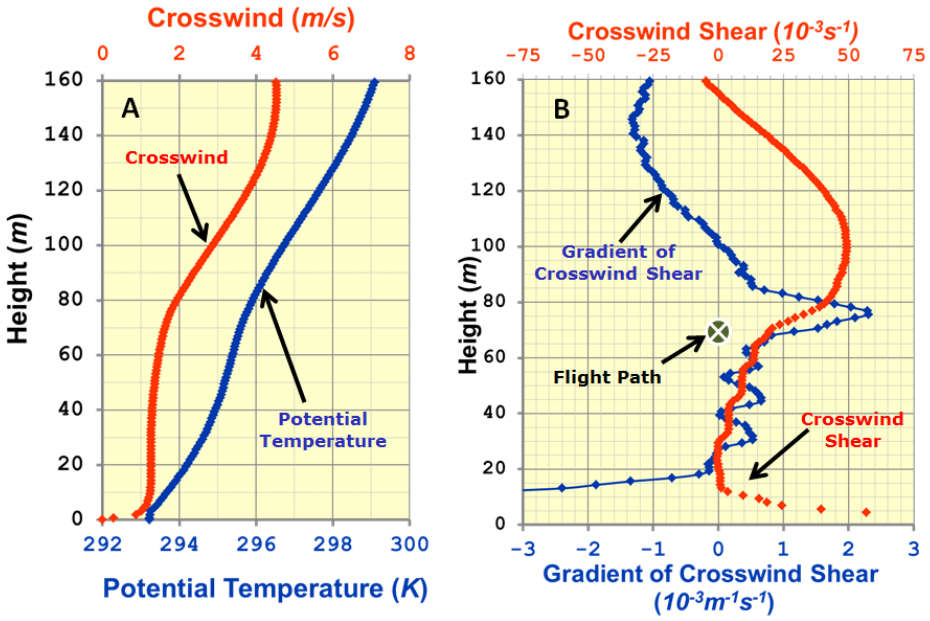

Figure 5. Enviornmental crosswind and potential temperature profile for Idaho Falls Run 23 case are depicted in (A). The crosswind shear and vertical gradient of the crosswind shear are shown in (B).

IV. Results

Three simulations are performed with the three-dimensional TASS model. Most of the results focus on the first simulation which uses the sounding in Fig. 5 for initial conditions. The two additional simulations were conducted to help clarify the wake's behavior in relation to the temperature and wind profiles. In one of the simulations, the

temperature is assumed to be adiabatic (constant potential temperature), and in the second, the mean crosswinds are assumed to be calm.

The vortex pair is initialized in the simulation at a height of 70*m*, which is near the elevation for the fly-by for the B-767 in the Idaho Falls Run 23. The positive vertical gradients of crosswind and crosswind shear (Fig. 5) affects the tilt of the vortex pair causing the port vortex (upstream) to tilt above the starboard vortex (downstream). From Fig. 6, we see that the port vortex descends at a slower rate and stays at a higher elevation than the starboard vortex. Specifically, the port vortex reaches a minimum height of 38*m* (Z^* = 0.75) at 48*s* (T^*=1.73), while the starboard vortex descends to a lower minimum height of 25*m* (Z^*=0.50) at 43*s* (T^*=1.55). Both vortices exhibit a single rebound, and then ascend through the remainder of their lifetime. The circulation of the starboard (downstream) vortex decays rapidly relative to the port (Fig. 7). The lifetime of the starboard vortex is about 2 minutes, while the port vortex has a lifetime of over 4 minutes! Assuming a detection threshold of 100 m^2s^{-1}, the port vortex survives an additional 2*min* and 45*s* as an isolated vortex. Note that the circulation of the port vortex is over 400 m^2s^{-1} at the time the starboard vortex dissipates to less than 75 m^2s^{-1}.

The values of circulation are re-plotted in nondimensional units in Fig. 8. Assuming a threshold for detection of Γ^* = 0.2 (~113m^2s^{-1}): the starboard vortex lifetime is T^* = 2.9, while port vortex lifetime is T^* = 8.8; thus, the duration of the port vortex is about three times that of the starboard.

Additional simulations were performed to verify that the long-lasting wake vortex behavior was indeed due to the crosswind shear. In the absence of crosswind shear, both vortices descend at the same rate, and have typical lifetimes for IGE vortices. In another experiment the crosswinds are retained, but the initial temperature profiles is changed to adiabatic. The circulation decay for this modified environment is included in Fig. 8. It shows that the neutral atmosphere affects the rate of decay (now even longer lasting), but still follows the same behavior as the original experiment.

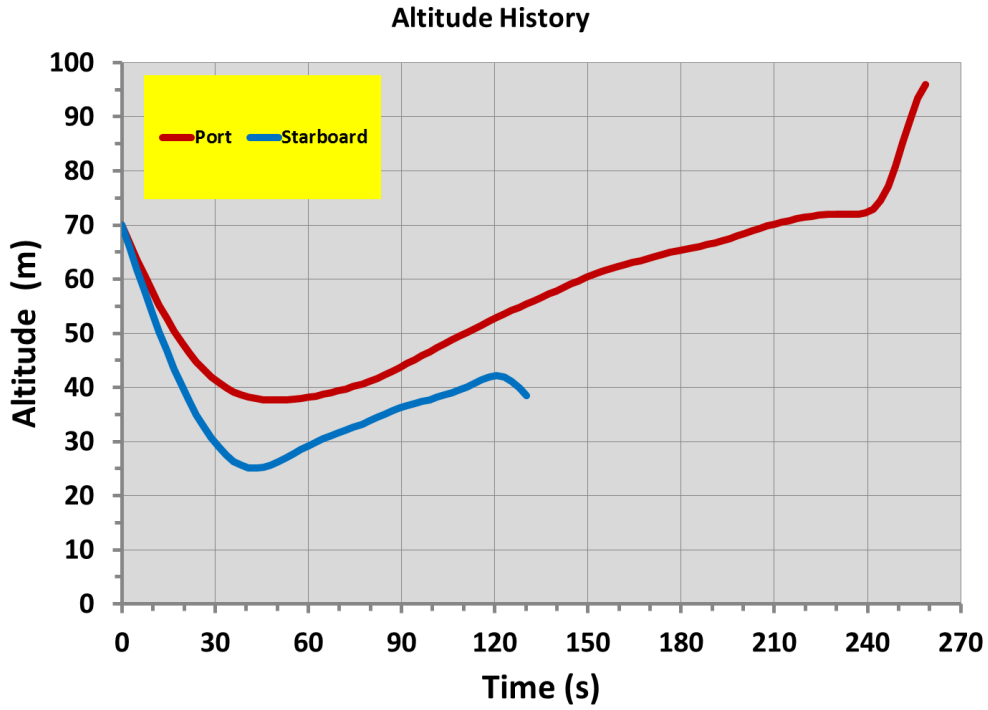

Figure 6. Altitude history for port and starbord vortices from numerical simulation using the sounding in Fig. 5 as input. The port vortex is upstream from the starboard vortex.

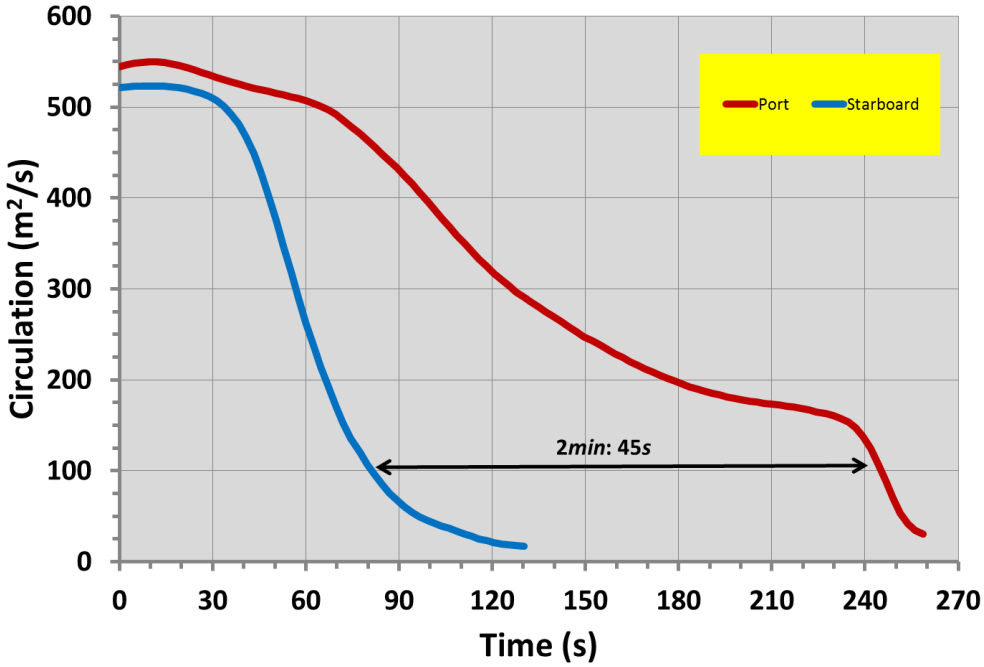

Figure 7. Circulation history for port and starbord vortices from numerical simulation using the sounding in Fig. 5 as input.

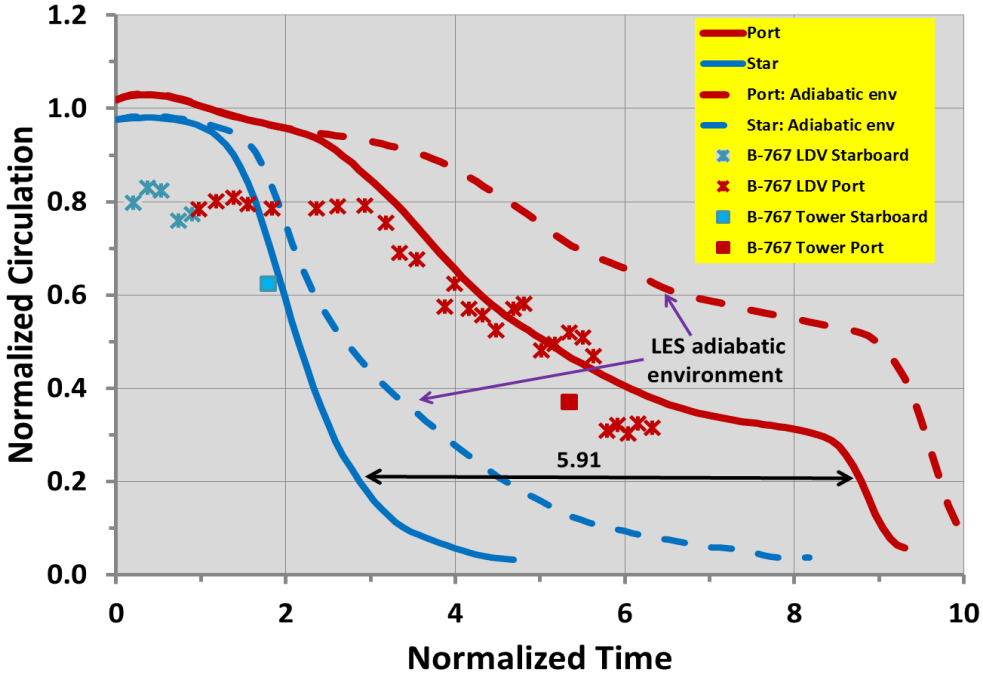

Figure 8 Nondimensional circulation vs nondimensional time. Numerical circulation histories for Run 23 environment represented by solid line; histories from simulation with initial condition modified for adiabatic temperature profile shown as dashed line. Normalized 10*m*-average circulations from measurements of the B-767 wake with LDV Lidar and tower are depicted as symbols.

As expected the normalized values of circulation measurements obtained at Idaho Fall for a B-767 fly-by are close to the normalized circulation results from our numerical simulations assuming the wake of a B-747, (Fig. 8). Also as the model results suggest, the starboard vortex may have been detected only a limited time due to its rapid weakening. The LDV Lidar was able to track the downstream (starboard) vortex only until $T^* = 1.45$. Shortly after this last detection by Lidar, the starboard vortex passed through the tower, where it had lost 39% of its strength ($T^* = 1.8$). The apparently longer-lived upstream (port) vortex was tracked by Lidar through $T^* = 6.32$, and showed very good agreement with the numerical simulation.

A comparison of Fig. 8 with the bounding curve representing many IGE measurements (as in Fig. 2) demonstrates that crosswinds can lead to abnormally long wake vortex lifetimes. It is one of the goals of this study to help better understand conditions that may lead to unusual events that could impact the safety of National Airspace Operations.

A visualization of the three-dimensional vortex isosurfaces (Fig. 9) illustrates the decay process for the isolated long-lived vortex event. Figure 9A shows the vortex pair at the time of minimum descent ($T^*=1.55$), and just before the beginning of rapid decay of the starboard (downstream) vortex. Note that the vortex pair tilts upward into the upwind direction. Also apparent is the onset of turbulence, manifesting itself as tubes tangentially wrapping around the starboard vortex. By $T^* = 2.24$ (Fig. 9B), the starboard vortex has become immersed in self-generated turbulence and has decayed to ~80% of its initial value. At the same time the port vortex has not yet undergone significant decay. By $T^* = 3.56$ (Fig. 9C), the port vortex is undergoing a more rapid decay, and only a region of residual turbulence remains of the starboard vortex.

Summarizing the transport and decay process from this study, the positive gradient of crosswind shear causes the port vortex to descend slower and rebound at a slightly later time than the starboard vortex. Interaction of the starboard vortex with a crosswind having a positive vertical derivative causes the starboard vortex to rapidly decay. At some later point in time, the port vortex begins a more rapid decay. Both vortices ascend after rebound, with the port persisting a greater period of time. The early demise of starboard vortex, and slower decay of the port vortex, allows the port vortex to become an isolated long-lived vortex.

V. Conclusion

A long-lasting wake vortex is simulated in ground effect using the TASS model. One of the members of the vortex pair decays at a much faster rate leaving a solitary vortex that persists almost three times longer than the shorter-lived member. The long lifetime, tilting of the wake pair, and differential decay rates can be attributed to the characteristics of the vertical profile for crosswinds. The second vertical derivative of crosswind affects the tilt of the vortex pair, while the first vertical derivative affects the decay rate. The results from numerical simulations of this event support the predictions in Table 1.

The effects from crosswind are important and should be included in wake vortex prediction models to account for uncertainties in vortex strength and position that may arise from crosswind shear. A technical challenge will be the development of sensors and sensor processing software that will detect crosswinds with sufficient resolution and accuracy to obtain the derivatives needed for predicting wake behavior.

A)

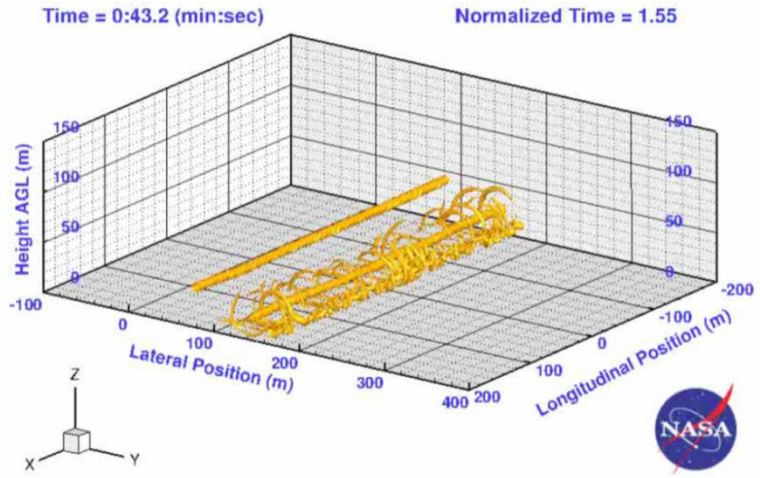

B)

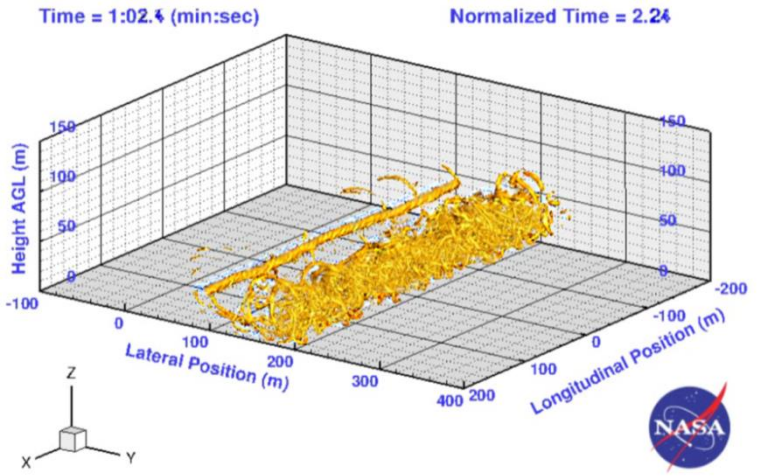

C)

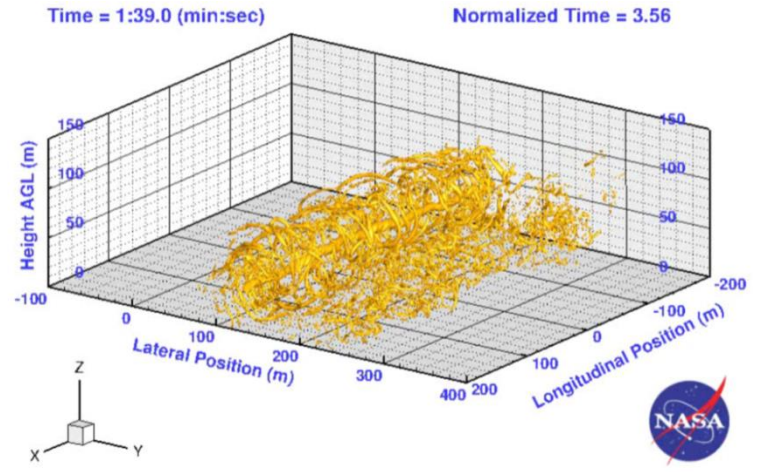

Figure 9. Three dimensional visualization of simulated wake vortex pair in the Idaho Falls Run 23 environment at three different times during its evolution: A) time when starboard vortex reaches minimum altitude and enhanced IGE decay begins, B) rapid decay phase for starboard vortex, C) demise of starboard vortex and enhanced decay of port vortex. Isosurfaces shown in the figures represent the eigenvalue of the velocity gradient tensor.[22]

Acknowledgments

This work is sponsored under NASA's Concepts & Technology Development Project of the Airspace Systems Program. I would like to thank Mr. Jeffery Tittsworth, (FAA Wake Turbulence program manager) for providing the data for Figs. 3 and 4. Also, I wish to thank Mr. Randal VanValkenburg (Flight Software Systems Branch) and Mr. George Switzer (NASA LITES Contractor) for their vital contributions. Lidar measurements from Idaho Falls are courtesy of Volpe National Transportation Center. Data sharing with the FAA was under Interagency Agreement IA1-1325, Annex 1. The numerical simulations were conducted using the NASA Pleiades supercomputer cluster.

References

[1]Connel, L., and A. Jakey, "Wake Vortex Encounters Study Update from NASA ASRS," Wakenet USA, Powerpoint Presentation, March 26, 2014, 55 pgs.

[2]Proctor, F.H., Hamilton, D.W. and Han, J., "Wake Vortex Transport and Decay in Ground Effect: Vortex Linking with the Ground," January 2000, AIAA-2000-0757.

[3]Robins, R. E., Delisi, D.P., and Greene, G.C., "Algorithms for Prediction of Trailing Vortex Evolution," *Journal of Aircraft*, Vol. 38, No. 5, September-October 2001, pp. 911-917.

[4]Delisi, D., and Lang S., "Presentation on Wake Turbulence Re-Categorization Phase I Methodology and Safety Case," Wakenet-Europe, RECAT Workshop, Berlin, Germany, Powerpoint Presentation, 20 June 2011 (http://www.wakenet3-europe.org/index.php?id=180).

[5]Proctor, F.H., and Ahmad, N.N., "Crosswind Shear Gradient Affect on Wake Vortices," June 2011, AIAA 2011-3038.

[6]Brashears, M.R., Logan, N.A. and Hallock, J.N., "Effect of Wind Shear and Ground Plane on Aircraft Wake Vortices," *J. Aircraft*, Vol. **12**, 1975, pp. 830-833.

[7]Garodz, L.J., and Clawson, K.L., "Vortex Wake Characteristics of B757-200 and B767-200 Aircraft Using the Tower Fly-By Technique, Volumes 1 and 2," January 1993, NOAA Tech. Memo. ERL ARL-199.

[8]Proctor, F.H., "Numerical Simulation of Wake Vortices Measured During the Idaho Falls and Memphis Field Programs," 14th AIAA Applied Aerodynamic Conference, Proceedings, Part II, June 1996, AIAA 96-2496, pp. 943-960.

[9]Proctor, F.H., and Hamilton, D.W., "Evaluation of Fast-Time Wake Vortex Prediction Models," January 2009, AIAA-2009-344.

[10]Systems Research Corporation, "Atmospheric Description for Idaho Falls B-757 Run #9 on September 25, 1990," Volpe National Transportation Systems, Cambridge, MA, Jan. 1994.

[11]Proctor, F.H., "The Terminal Area Simulation System, Volume 1: Theoretical Formulation," April 1987, NASA CR-4046.

[12]Han, J., Lin, Y. -L., Schowalter, D. G., Arya, S. P., and Proctor, F. H., "Large Eddy Simulation of Aircraft Wake Vortices within Homogeneous Turbulence: Crow Instability," *AIAA Journal*, Vol. 38, No. 2, February. 2000, pp. 292-300.

[13]Proctor, F.H., "Interaction of Aircraft Wakes from Laterally Spaced Aircraft," January 2009, AIAA 2009-0343.

[14]Switzer, G., and Proctor, F., "Terminal Area Simulation System User's Guide Version 10.0," December 2013, NASA TM-2014-218050.

[15]Proctor, F.H., and Han, J., "Numerical Study of Wake Vortex Interaction with the Ground Using the Terminal Area Simulation System," January 1999, AIAA 99-0754.

[16]Leonard, B. P., M. K. MacVean and A. P. Lock, "The Flux-Integral Method for Multidimensional Convection and Diffusion," *Applied Mathematical Modeling*, Vol. 19, 1995, pp. 333-342.

[17]van Leer, B., "Towards the Ultimate Conservative Difference Scheme: V, A Second-Order Sequel to Godunov's Method," *Journal of Computational Physics*, Vol. 32, 1979, pp. 101-136.

[18]Ahmad, N.N., and Proctor, F.H., "Advection of Microphysical Scalars in Terminal Area Simulation System (TASS)," AIAA 2011-1004.

[19]Arakawa, A., and Lamb, V.R., "Computational Design of the Basic Dynamical Process of the UCLA General Circulation Model," *Methods in Computational Physics*, Vol. 17, 1977, pp. 173-265.

[20]Klemp, J. B., and Wilhelmson, R., "The Simulation of Three-Dimensional Convective Storm Dynamics," *Journal of Atmospheric Sciences*, Vol. 35, June 1978, pp. 1070-1096.

[21]Switzer, G.F., "Validation Tests of TASS for Application to 3-D Vortex Simulations," October 1996, NASA CR-4756.

[22]Jeong, J., and Hussain F., "On the Identification of a Vortex," *Journal of Fluid Mechanics*, Vol. 285, 1995, pp. 69-94.